FINAL REPORT

Project Title: Spatial and Temporal Mapping of ^{10}B Distribution in Vivo Using Nuclear Reactor-Based Prompt Gamma Neutron Activation Analysis and Image Reconstruction Techniques

Covering Period: July 1, 2002 through December 31, 2005

Date of Report: 22 May 2006

Recipient: Massachusetts Instituted of Technology, Cambridge, MA 02139

Award Number: DE-FG07-02ID14343

Subcontractors: None

Contact(s): Jacquelyn C. Yanch
NW14-2207 Massachusetts Institute of Technology,
Cambridge, MA 02139
jcyanch@mit.edu
(617)248-6999
(617)253-0760 (fax)

Project Objective:

This project involved the development of a method for *in vivo* prompt gamma neutron activation analysis for the investigation of Boron-10 distribution in a rabbit knee. The overall objective of this work was a robust approach for rapid screening of new ^{10}B-labelled compounds to determine their suitability for use in the treatment of rheumatoid arthritis via Boron Neutron Capture Synovectomy (BNCS).

For BNCS it is essential to obtain a compound showing high uptake levels in the synovium and long residence time in the joints. Previously the in vivo uptake behavior of potential compounds was evaluated in the arthritic knee joints of rabbits via extensive dissection studies. These studies are very labor-intensive and involve sacrificing large numbers of animals. An *in vivo* ^{10}B screening approach was developed to provide initial evaluation of potential compounds. Only those compounds showing positive uptake and retention characteristics will be evaluated further via dissection studies. No further studies will be performed with compounds showing rapid clearance and/or low synovial uptake.

Two approaches to in vivo screening were investigated using both simulation methods and experimentation. Both make use of neutron beams generated at the MIT Research Reactor. The first, Transmission Computed Tomography (TCT) was developed and tested but was eventually rejected due to very limited spatial resolution using existing reactor beams. The second, in vivo prompt gamma neutron activation analysis (IVPGNAA) was much more promising. IVPGNAA was developed using computer simulation and physical measurement coupled with image reconstruction techniques. The method was tested in arthritic New Zealand rabbits previously injected intra-articularly with three boron labeled compounds and shown to be effective in providing information regarding uptake level and residence time of ^{10}B in the joint.

1. Background

Rheumatoid Arthritis (RA) is an autoimmune disease characterized by swollen, inflamed and painful joints. The inflammation of the synovial membrane (synovium) lining the joint is the source of pain and disability. The cause of RA is unknown, and there is as yet no cure. The primary treatment for the symptoms of RA consists of using various drugs to reduce synovial inflammation (Harris 2001). For those joints unresponsive to anti-inflammatory drugs, synovectomy, the procedure of physically removing or ablating the inflamed membrane, becomes necessary to both alleviate symptoms and to protect cartilage and bone from eventual destruction (Newman et al 1994).

Because of the general dangers of surgery and the prolonged rehabilitation associated with surgical synovectomy, alternatives have been sought. Radiation synovectomy is performed by injecting beta-emitting radionuclides directly into the joint. The beta particles deposit most of their energy locally thereby destroying the diseased synovium (Shortkroff et al 1993). It has been shown that radiation synovectomy is equally as effective in reducing the symptoms of RA as surgery, and is much easier to perform. It is widely used in Europe, Australia, and Canada. However, leakage of the radionuclides from the joint causes healthy tissue irradiation, and dose to regional lymph nodes is of special concern. For this reason, radiation synovectomy is not approved for routine clinical use in the United States.

Another alternative treatment modality, Boron Neutron Capture Synovectomy (BNCS), is currently under investigation (Yanch et al 1999). BNCS is a two-part procedure involving a direct injection of a non-radioactive, boronated compound into the affected joint followed by irradiation of the joint with low energy neutrons. The nuclide ^{10}B has a high thermal neutron capture cross section. When the joint is irradiated with a low energy neutron beam, the $^{10}B(n,\square)^{7}Li$ reaction delivers a large, high LET and high RBE dose locally to the ^{10}B-loaded synovium, thereby destroying the diseased membrane. Like radiation synovectomy, BNCS eliminates the necessity and associated dangers of open surgery, is easy to perform, and can greatly reduce rehabilitation time. Unlike radiation synovectomy, as the radiation dose is only delivered during neutron irradiation, the radiation hazard caused by leakage of injected compound is eliminated.

The efficacy of BNCS was initially tested in an Antigen-induced Arthritis (AIA) animal model using the ^{10}B-enriched compound $K_2B_{12}H_{12}$. Prior dissection studies had demonstrated that injection of a solution containing 150,000 ppm ^{10}B resulted in average synovium ^{10}B concentrations of 19,000 ppm for 30 minutes post-injection (Binello 1999). Extensive synovial necrosis was observed after the delivery of a radiation dose of 10,000 RBE-cGy or higher. It was thus demonstrated that BNCS is effective in ablating the synovium and therefore in treating the symptoms of rheumatoid arthritis (Shortkroff et al 2003).

However, the residence time of $K_2B_{12}H_{12}$ in the joint is very short (Binello 1999), and animal experiments showed that this compound is also able to enter the articular cartilage, resulting in extensive cartilage damage upon neutron irradiation (Shortkroff et al 2003). Therefore, it is necessary to find a new compound for eventual use with RA patients.

Any potential compound for BNCS must be fully evaluated for its in vivo uptake behavior in the synovium. To date, the in vivo uptake behavior of a small number of alternative compounds has been investigated using the AIA model in the knee joints of the New Zealand white rabbit (Binello 1999). Information regarding the uptake, spatial position, and time course of potential compounds in synovial tissue is obtained via extensive dissection studies. For these studies, animals are anesthetized and the compound is directly injected into the synovial fluid of the knee. At each of several time points following injection, several animals are sacrificed and the knee joints carefully dissected from the subcutaneous tissues and surrounding muscles. Several samples of synovium, synovial fluid, and other joint tissues are removed from each animal and frozen. The ^{10}B concentration in these samples is then determined via Prompt Gamma Neutron Activation Analysis at the 4DH3 beam port at the Massachusetts Institute of Technology Research Reactor (MITR).

The dissection study is a reliable technique for evaluation of the temporal and spatial uptake characteristics of a compound in vivo. However, it is also extremely costly and labor- intensive. The mapping of the uptake time course of a compound requires the sacrificing and careful dissection of statistically significant numbers of animals at several time points post-injection, therefore very large numbers of animals are required.

An in vivo ^{10}B mapping technique used as a screening approach could dramatically reduce the number of animals needed for compound evaluation. Dissection studies showed that some compounds, such as boron metal particulate, coagulate in the synovial fluid and do not disperse to other regions within the joint even after 24 hours; some others, such as the $K_2B_{12}H_{12}$, redistribute throughout the knee quickly and leave the joint within 60 minutes (Binello 1999). If the information regarding the compound redistribution time course could be determined using an in vivo ^{10}B mapping technique performed on a single living animal, it would allow rejection of some compounds at the screening phase, leaving only those with reasonable longevity and distribution characteristics for more costly and time-consuming dissection studies. There may even be the potential of using the same animal in the evaluation of more than one compound.

1.1 Transmission Computed Tomography

Our first approach examined the potential of transmission computed tomography (TCT) for the in vivo evaluation of ^{10}B distribution in a rabbit knee (Zhu et al 2002). TCT uses a parallel neutron beam to irradiate the rabbit knee. The neutron intensity transmitted through the knee is then recorded as one two dimensional projection by a ^{6}LiF-ZnS scintillation screen -- CCD camera system (Lanza et al 1996) placed after the knee. The animal is then rotated through some angle and the next projection is recorded. The neutron absorption rates calculated for all the projections are then used to reconstruct a spatial map of neutron absorption coefficients in the knee. Because ^{10}B has a significantly higher thermal neutron absorption cross section than average tissue material in a rabbit knee, the neutron absorption coefficient map could be used for ^{10}B spatial distribution quantification in the knee.

The TCT approach was first tested using simulated projection data generated by modeling a thermal neutron beam incident on a rabbit knee phantom using the Monte-Carlo N-Particle (MCNP) transport code (Briesmeister 1997). Reconstruction results using simulation data suggested that TCT is promising for the in vivo ^{10}B screening in a rabbit knee with an estimated minimum flux of thermal neutrons of 10^7 n/cm^{2}s. Two beam ports at the MITR have been considered as potential neutron sources for TCT. The 4DH3 beam port delivers a clean, diffracted, 0.015 eV neutron beam with a flux of 1.7×10^7 n/cm^{2}s (Riley and Harling 1998). The beam diameter is 2.54 cm, which is comparable to the size of a typical rabbit knee. However, because of its low energy, the neutron transmission rate through the knee is about two orders of magnitude lower than that expected with a thermal (0.025 eV) beam. Subsequent TCT experiments performed at the 4DH3 beam port using a water-filled rabbit knee phantom confirmed that no quantitative or spatial information could be obtained from the resulting image. To effectively use TCT for in vivo ^{10}B screening, a neutron source with higher intensity and/or higher average neutron energy is desirable. Another potential source, the M11 beam port of the MITR, has a much higher thermal neutron flux (approximately 5×10^9 n/cm^{2}s when the reactor is operating at a full power). However, because of its large beam size (12 cm diameter) and high fast neutron and photon contamination level, the expense of modifying the M11 beam for in vivo boron analysis would be considerable. Therefore, an alternative approach making use of the 4DH3 beam, the 'in vivo prompt gamma neutron activation analysis' (IVPGNAA) approach, was investigated.

1.2 In Vivo Prompt Gamma Neutron Activation Analysis

Prompt gamma neutron activation analysis (PGNAA) has been used extensively in Boron Neutron Capture Therapy (BNCT) research to determine boron concentrations in blood and tissue samples. In 94% of the neutron capture reactions in ^{10}B, the ^7Li nucleus is left in an excited state, which de-excites by emission of a 478 keV gamma photon immediately after the capture reaction. To perform PGNAA, a small sample is placed in a teflon vial and positioned in a neutron beam. A high-purity germanium detector collects a prompt gamma spectrum, from which the areas of the 478 keV photon peak and the 2.2 MeV photon peak from the $^1H(n,\gamma)^2H$ reactions are determined. The ratio of the two peak areas is compared with a calibration curve constructed using boric acid standards, and the ^{10}B concentration in the sample is thereby obtained.

A typical PGNAA measurement does not provide information regarding ^{10}B distribution within the sample. However, if a narrow neutron beam is used, it would be possible to obtain a certain degree of spatial information regarding boron content in a live rabbit knee. Because of the high hydrogen content in animal tissues, low energy neutrons can be easily scattered to other parts of the knee. However, when a narrow neutron beam is used, the neutron density in the region around the point of incidence is much higher than in other parts of the knee. This is illustrated in Figure 1 which plots MCNP-simulated two-dimensional neutron iso-flux contours resulting from a 3.5 mm wide, 0.015 eV neutron beam incident upon a water-filled elliptical cylinder of the size of a typical rabbit knee. The neutron flux falls to 50% at

a depth of approximately 4 mm in water, and to 10% at a depth of around 1 cm. Because of the partially localized neutron distribution, a given amount of ^{10}B located in different regions within the knee will make different contributions to the 478 keV gamma signal. Therefore, if the rabbit knee is rotated so that the 478 keV gamma signal can be collected from several different angular positions, a two dimensional ^{10}B distribution map in the knee can be reconstructed by solving a group of simultaneous equations. In addition, by repeating this procedure post injection, a time course of the compound distribution can be obtained in vivo without sacrificing the animal.

To investigate the practical feasibility of this approach in a geometry similar to the rabbit knee joint, computer simulations were performed. The IVPGNAA system, including a rabbit knee phantom with varied ^{10}B distributions, a neutron beam and a detector surface, was modeled within the MCNP code, and projection data from several angular positions were generated by separate runs. The MCNP generated data were then reconstructed into a two dimensional ^{10}B distribution map, and compared with the original distribution. The effects of variations in the anatomy of individual rabbit knees, and the effects of positioning errors on the reconstruction results were quantified.

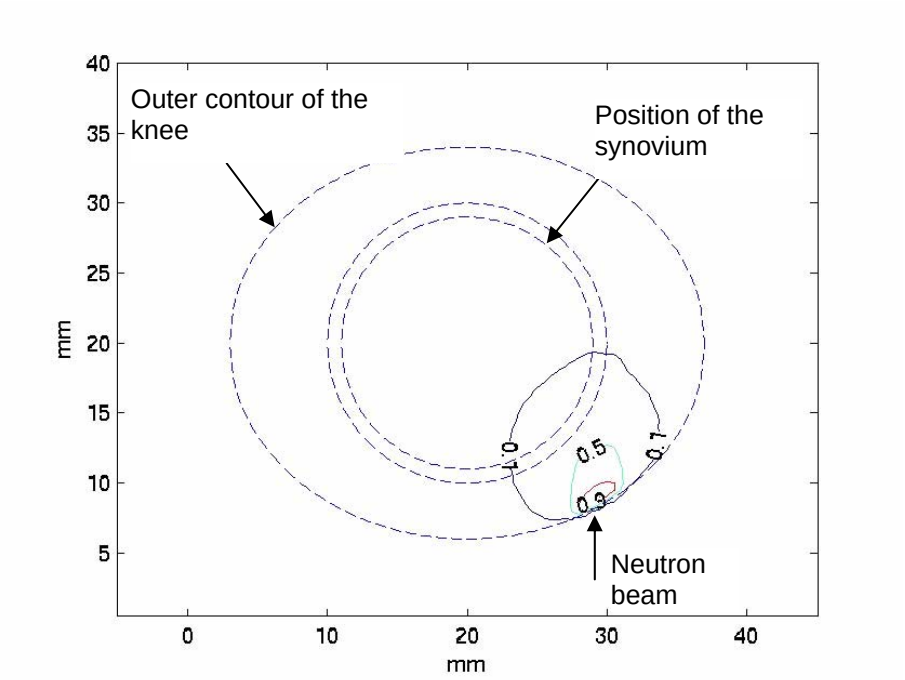

Figure 1. Iso-flux contours of a narrow neutron beam incident on a water-filled, rabbit knee-shaped elliptical cylinder, obtained via MCNP simulation. The beam is 3.5 mm wide. The neutron energy is 0.015 eV. The dashed curves show the outer contour of the knee and the position of the synovium. The neutron distribution is partially localized around the point of incidence, dropping to 50% at a depth of 4 mm, and to 10% at a depth of 1 cm.

2. Method - Simulations

IVPGNAA will be performed using the 4DH3 neutron beam from the MIT Research Reactor (MITR). This beam port currently houses the PGNAA facility of the MITR and is used regularly, among other applications, for the quantification of boron in blood samples from subjects participating in clinical

trials of Boron Neutron Capture Therapy (BNCT) for the treatment of brain tumors (Newton et al 2002). The 4DH3 beam is well collimated, 25.4 mm in diameter, and renders a mono-energetic (0.015 eV) neutron beam via selective diffraction off a set of single graphite crystals located upstream of the experiment area (Riley and Harling 1998).

Because of the open space needed for the rotation of the animal, the rabbit knee position for IVPGNAA is 120 cm down-stream from the beam aperture. Also, since the size of the 4DH3 beam is similar to the diameter of a rabbit knee, spatial resolution of differences in ^{10}B concentration within the knee will not be possible unless the beam is substantially collimated. A 15 cm long collimator made of ^{6}LiF-loaded epoxy narrows the beam down to 3.5 mm × 20 mm vertically. With the collimator in place, the neutron flux at the knee position is 8.5×10^5 n/cm^{2}s, as measured by the gold foil activation technique.

2.1. Proposed experimental approach

A schematic illustration of the proposed experimental set up for IVPGNAA is shown in Figure 2. An AIA rabbit will be placed on a rotatable aluminum stand with the knee to be irradiated suspended in the neutron beam, 120 cm from the beam aperture. The collimator is placed between the knee and the beam opening, 40 cm from the knee. A germanium detector is placed adjacent to the knee and compound, direction. Immediately after the intra- articular injection of a boron-labeled the anesthetized animal will be secured perpendicular to the beam on the aluminum stand with the leg positioned in the beam. A prompt gamma spectrum will be collected during a 1 to 2 minute neutron irradiation. The net peak area and uncertainty of the 478 keV photons from the ^{10}B capture reaction will be recorded. The animal will then be turned 360/*m* degrees and a second spectrum will be obtained. This process will be repeated *m* times until all projection data are collected.

To reconstruct the ^{10}B distribution from the *m* projections, the ^{10}B-containing region of the knee is divided into *n* compartments. The probability of a given amount of ^{10}B in each compartment contributing to the photon signal at the detector, for each angular position, is estimated by Monte Carlo simulation. The ^{10}B concentration in each compartment is then obtained by solving a set of simultaneous equations.

Because the synovium is in immediate contact with the synovial fluid into which the boron-labeled compound is injected, the boron concentration measured in the synovium is very much larger than that measured in other joint tissues (often by several orders of magnitude). This has been confirmed by previous dissection studies involving several different compounds (Binello 1999). Therefore, in the simulation study described here, ^{10}B is assumed to exist only in the synovium and/or the synovial fluid.

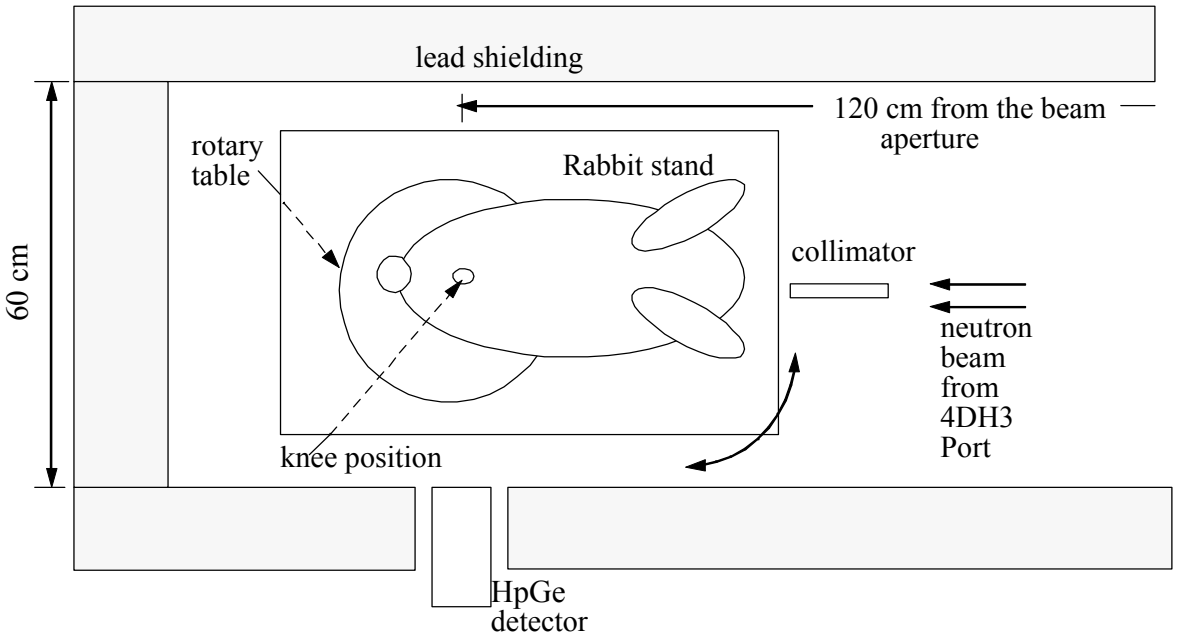

Figure 2. Schematic illustration of the experimental setup proposed for IVPGNAA. The neutron beam from the 4DH3 beam port of the MIT research reactor is narrowed down by a collimator, then incident on a rabbit knee. The rabbit is placed on an aluminum stand with the knee hanging down in the beam. The stand is placed on a rotary table. A high-purity germanium detector collects the 478 keV gamma signal emitted from the $^{10}B(n,\alpha)^{7}Li$ reactions.

2.2. MCNP simulation of the experimental approach

The Monte Carlo N-Particle (MCNP) radiation simulation code is a state-of-the-art, general-purpose, continuous-energy Monte Carlo transport code system. It can be used for neutron, photon, electron, or coupled neutron/photon/electron transport in a three dimensional heterogeneous configuration of materials. Point wise cross-section data are used. MCNP features a powerful general source, a flexible tally structure, and an extensive collection of cross-section data (Briesmeister 1997).

To investigate the feasibility of the IVPGNAA approach, the experimental set up for IVPGNAA shown in Figure 2 was modeled within the MCNP code (Version 4B) to generate simulated projection data. The neutron source was modeled as a 3.5 mm × 20 mm mono-directional, mono-energetic (0.015 eV) surface source. A rabbit knee phantom was designed based on MRI images of AIA rabbit knees, and modeled within MCNP. The detector was modeled as a surface 5 cm in diameter. The 478 keV gamma photons incident upon this surface were tallied as the projection data. The *m* projection data for each ^{10}B distribution were generated by *m* separate MCNP runs with different knee/beam orientations.

2.3. Rabbit knee model

Using MRI images of rabbit knees made arthritic with the AIA approach, a rabbit knee phantom was constructed within the MCNP code, as shown in Figure 3. The model comprises an elliptical cylinder with major and minor axes of 34 mm and 28 mm. The synovial membrane (synovium), which lines the inner joint capsule, is 1 mm thick and 20 mm in diameter at its thickest and is tapered as it joins the femur

and tibia. The distance between the two bone surfaces is 2 mm. The space bounded by the synovium and the two bone surfaces is filled with synovial fluid. The entire ^{10}B containing region of the knee, including the synovium and synovial fluid, is evenly partitioned into *n* compartments. Tissue compositions were based on the recommendations of the ICRU [1989].

In a live animal, as in a human patient, the boron-labeled compound would be injected into the synovial fluid, then would be taken up phagocyticly or diffuse into the synovium. Information regarding the time course of the uptake level and the extent to which the uptake is homogeneous around the knee is the goal of IVPGNAA.

2.4. Reconstruction

To reconstruct the ^{10}B distribution in the knee, an $m \times n$ probability matrix, *A,* is first generated. Matrix *A* contains the probability that a unit amount of ^{10}B will contribute to the photon signal at the detector, from each compartment, for each angular position. Entries of the probability matrix

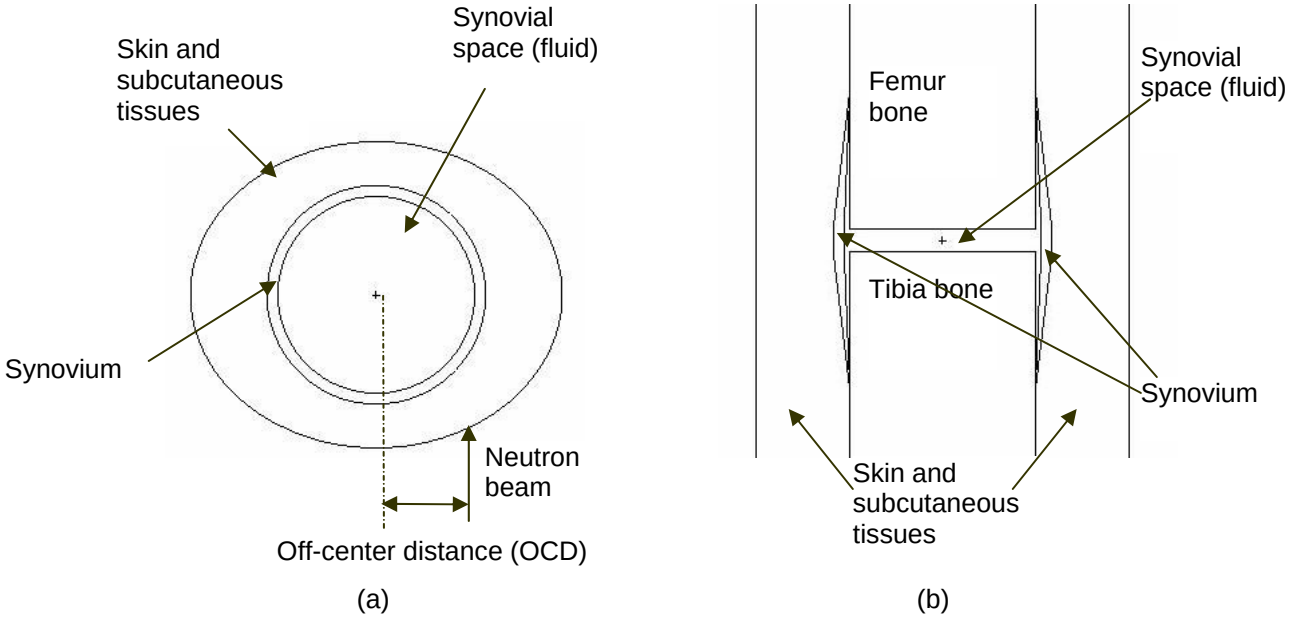

Figure 3. The AIA rabbit knee phantom modeled in MCNP. (a) Cross-section through the synovial space. (b) Sagittal view of the AIA rabbit knee model. The knee is modeled as an elliptical cylinder with major and minor axes of 34 mm and 28 mm respectively. The synovium is 1 mm thick and 20 mm in diameter at its thickest. It is tapered as it joins the femur and tibia. The distance between the two bone surfaces is 2 mm. The space bounded by the synovium and the two bone surfaces is filled with synovial fluid.

can be approximated by the neutron fluxes in each compartment at each angular position. For a compartment j (j = 1, …, n) at angular position i (i = 1, …, m), if the neutron flux in the compartment is Φ_{ij}, then the number of 478 keV photons emitted from j is proportional to $\Phi_{ij} V_j \sigma [^{10}B]_j$, where V_j is the volume of compartment j; $[^{10}B]_j$ is the ^{10}B concentration in the compartment, and σ is the average cross

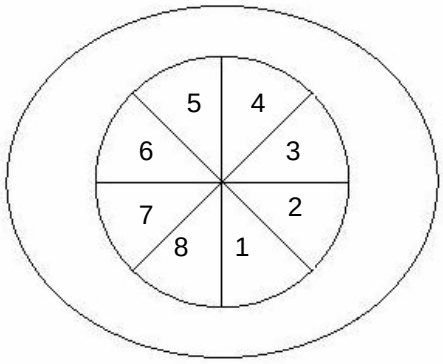

Figure 4. Partition of the ^{10}B-containing region of the knee. The ^{10}B containing region of the knee (synovium and fluid) is evenly divided into 8 compartments.

section of the $^{10}B(n,\alpha)^{7}Li$ reaction. When the synovium is evenly partitioned, all the compartments have the same volume, *V*. Assuming a constant cross section with neutron energy (see below), the probability of a given ^{10}B concentration contributing to the 478 keV photon signal is proportional to the neutron flux in compartment Φ_{ij}.

The probability matrix, *A,* was generated by MCNP simulation. The neutron fluxes in *n* compartments at *m* different angular positions were tallied using volume tallies in *m* separate runs. Because the energy of the incident neutron beam is slightly lower than the energy distribution obtained at room temperature, some amount of up scattering will occur within the knee. Thus, neutrons in compartments further away from the point of incidence have a slightly higher average energy, therefore a lower cross section, than neutrons in compartments closer to the beam. This factor can be corrected for by modifying each probability entry with a factor, $1/\sqrt{E_{ij}}$, where E_{ij} is the average neutron energy in the compartments as determined by the MCNP simulation.

After the probability matrix is obtained, a reconstruction of the ^{10}B distribution in the knee can be found by solving the following set of simultaneous equations

$$Ax = b\,, \qquad (1)$$

where *A* is the $m \times n$ probability matrix, *x* is an $n \times 1$ vector representing the relative ^{10}B concentrations in *n* compartments, and *b* is an $m \times 1$ vector representing the projection data from *m* different angular positions. For $n = 8$ compartments and $m = 16$ angular positions, the condition number of a simulation generated matrix *A* was found to be 12.2. Therefore, Equation (1) represents a stable over-determined system. As there is generally no exact solution to the over-determined system (1), the goal of reconstruction is to find the best estimate, $\hat{x}$, of the ^{10}B distribution.

The widely used least squares (LS) estimation minimizes the norm of a residual vector, $\|r\|$, where

$$r = b - A\hat{x}\ .$$

However, the entries in the measured projection vector, *b,* will be associated with a large range of uncertainties, indicating that some data points are more reliable than others. The weighted least squares (WLS) algorithm is able to attach more weight to more reliable measurements in a systematic way. Instead of minimizing $\|r\|^2 = (b - A\hat{x})^T (b - A\hat{x}) = r_1^2 + r_2^2 + \cdots$, WLS seeks to minimize $\|wr\|^2 = w_1^2 r_1^2 + w_2^2 r_2^2 + \cdots$, where w_i are the attached weights. Assuming the errors in b_i are independent, the weights can be chosen as $w_i = 1/\sigma_i$, where σ_i is the standard deviation of the measurement b_i in the projection vector, *b*. A small variance in b_i means a more reliable observation, therefore a larger weight. By attaching the weights, if b_i is trusted more than b_j, then r_i is made smaller. The WLS solution of (1) can be obtained by solving the normal equations:

$$(A^T C A)\hat{x}_{WLS} = (A^T C)b, \qquad (2)$$

in which $C = W^T W$. When the measurements are independent, the weight matrix, *W,* is a diagonal matrix with $W_{ii} = 1/\sigma_i$ (Strang 1986).

As the ^{10}B concentrations can not be negative in any of the compartments, it is reasonable to apply a non-negativity constraint:

$$x_i \geq 0, \; i = 1, \ldots, n.$$

When this constraint is applied, the solution is no longer a linear function of *b*. The non-negative least squares solution of a system can be calculated iteratively. An algorithm can be found in Lawson and Hanson (1974).

Based on above considerations, a non-negative weighted least squares (NNWLS) algorithm is used for the reconstruction of ^{10}B distributions in IVPGNAA. A weight matrix, *W*, is attached to equation (1) to form the WLS normal equations (2), which in turn are solved iteratively to obtain a NNWLS solution, $\hat{x}_{NNWLS}$.

2.5. Determination of the optimal off-center distance (OCD)

In order to detect the migration of the compound from the synovial fluid to the synovium, a difference of response between the synovium and synovial fluid is desirable so that boron in the synovium contributes more signal than that in the fluid. This difference may be improved by using an off-centered neutron beam, as illustrated in Figure 3. However, as the off-center distance (OCD) increases, the point of incidence moves closer to the edge of the knee, and the system may be more sensitive to errors in positioning of the rabbit knee. Therefore, the OCD of the neutron beam must be optimized.

To choose the optimal off-center distance, simulated probability matrices were generated for OCDs from 0 mm to 9 mm. To compare the relative contributions to the signal from the synovium and the synovial fluid, for each OCD, projection data were generated for two distributions, one with ^{10}B in only

the synovium portion of one section of the knee, the other with the same amount of ^{10}B in the same section but in the synovial fluid portion only. The ratios of the reconstructed values of these two cases were compared. To compare the sensitivity of the system to mis-positioning errors, for each OCD, projection data were generated for a ^{10}B distribution with mis-positioning errors from -2 mm to 2 mm. The standard deviations of reconstruction values of the compartments containing the same amount of ^{10}B were calculated. At the optimal OCD, the signal contribution from the synovium should be larger than that from the synovial fluid, and the deviation of reconstruction values caused by mis-positioning should be small.

2.6. Testing of the approach with simulations

The projection data of several potential ^{10}B distributions in the phantom were generated using MCNP simulation to test the effectiveness of the IVPGNAA approach. The ^{10}B containing region in the knee was partitioned into 8 compartments ($n = 8$), as shown in Figure 4. Projection data were generated for 16 angular positions ($m = 16$). The NNWLS algorithm was used to reconstruct the ^{10}B distributions.

Because of the variation in knee dimensions among different animals and the potential for errors in animal positioning, the knee dimensions and parameters (such as the OCD) modeled in generating the probability matrix might be slightly different from those of the actual animal and experiment. To test the effect of this inconsistency, some parameters were varied to generate projection data sets with characteristics that did not match those used to generate the probability matrix. The parameters varied included: the size of the knee (outer dimensions 1 to 2 mm larger or smaller), the depth of the synovium (1 or 2 mm deeper or shallower), the range of ^{10}B concentrations in the compartments (50 to 20,000 ppm), the off-center distance (1 or 2 mm larger or smaller), and the knee mis-positioning distance (1 or 2 mm to each side).

2.7. Estimates of uncertainty in boron concentration

The error vector e_{WLS} of the WLS solution, $\hat{x}_{WLS}$, can be estimated by calculating its covariance matrix:

$$P = (A^T C A)^{-1}, \tag{3}$$

where matrix C is the same as in (2). The square roots of the diagonal of P give e_{WLS}, the expected errors in $\hat{x}_{WLS}$ (Strang 1986). However, the errors in the NNWLS solution, $\hat{x}_{NNWLS}$, are difficult to calculate because the solution is a non-linear function of b. To obtain a realistic estimate of reconstruction uncertainties, projection data of several distributions under various conditions were generated using MCNP simulations. The standard deviations of compartments with the same ^{10}B concentrations were calculated, and then used as an estimate of uncertainty associated with reconstructed results.

3. Simulation Results

Probability matrix, *A*, was generated for the knee partition shown in Figure 4 using the AIA rabbit knee anatomic dimensions stated in Section 2.3. Projection data for several sample ^{10}B distributions under various conditions were also generated. The uncertainty level of projection data was in the range 3 – 7 %. Reconstructed distributions were compared with originals. The standard deviations of reconstructed values of all the compartments containing 2000 ppm ^{10}B were calculated as an estimate of the reconstruction uncertainty.

Compartment #	1	2	3	4	5	6	7	8
Distribution #1								
[B-10] (ppm)	100	2000	1000	2000	3000	2000	5000	2000
Reconstructed	0	2114	915	2096	2994	1716	4116	2099
Distribution #2								
[B-10] (ppm)	2000	2000	2000	2000	2000	2000	2000	2000
Reconstructed	2096	1894	1894	2092	2096	1893	1894	2092
Distribution #3								
[B-10] (ppm)	2000	0	0	0	0	0	0	0
Reconstructed	2417	0	0	7	0	0	0	4

Table 1. Reconstruction results of 3 sample ^{10}B distributions. The relative standard deviation of the reconstruction values of all the 2000 ppm compartments is 8.5% when the parameters used for generating the probability matrix match those used for generating projection data.

3.1. Results of reconstruction of several sample ^{10}B distributions

Table 1 shows the reconstruction results of three ^{10}B distributions. The synovial compartments are numbered as shown in Figure 4. The neutron beam is incident upon the center of the knee. All the results were normalized over the average reconstruction values of the four 2000 ppm compartments in Distributions #1 and 2. As shown in Table 1, when the parameters for generating the probability matrix match those for generating the projection data, the reconstruction results correctly reflect the ^{10}B distribution in the model. The relative standard deviation of the reconstruction values of all the 2000 ppm compartments in Distributions #1, 2 and 3 is 8.5%.

3.2 Determination of the optimal off-center distance (OCD)

Table 2 shows the relative contribution to the signal from the synovium and the synovial fluid for OCDs from 0 to 9 mm. For each OCD, projection data were generated for two cases. In both cases, the average ^{10}B concentrations in Compartments #1 and #2 are 1000 ppm. However, in the 'fluid' case, ^{10}B is located only in the synovial fluid portions of the compartments, while for the 'synovium' case, ^{10}B is located in the synovium portions. The ratios of the average reconstructed concentrations in Compartments #1 and #2 for the two cases are compared. Results indicate that when the OCD increases, there is no

significant difference between the contributions to the signal from the synovium and the synovial fluid.

[B-10] (ppm)		1000	1000	0	0	0	0	0	0	R_s/R_f
OCD = 1 mm	fluid	1183	998	90	0	43	62	35	70	1.18
	synovium	1431	1136	0	0	0	0	0	0	
OCD = 3 mm	fluid	1161	1021	47	58	20	74	7	99	1.18
	synovium	1420	1158	0	0	0	0	0	0	
OCD = 5 mm	fluid	1142	1021	51	42	32	3	39	107	1.19
	synovium	1575	1001	0	0	0	0	0	0	
OCD = 7 mm	fluid	1138	950	118	31	21	63	35	96	1.24
	synovium	1505	1103	0	0	0	0	0	0	
OCD = 9 mm	fluid	1106	975	150	0	52	46	55	68	1.26
	synovium	1543	1103	0	0	0	0	0	0	

Table 2. Ratios of contributions from synovium and from fluid for different OCDs. The same amount of ^{10}B is placed in the synovium or in the synovial fluid parts of the same compartments. The reconstructed values are compared. Within estimated levels of uncertainty of ~10%, as the OCD increases, there is no significant difference between the contributions to the signal from the synovium and the synovial fluid.

Table 3 shows the deviation of reconstructed values as a result of mis-positioning errors. For each of the OCDs from 0 to 9 mm, projection data for Distribution #1 (Table 1) were generated with mis-positioning distances (the distance between the center of the knee and the rotational axis of the system) of -2 mm, -1 mm, 0, 1 mm and 2 mm. The standard deviations of the reconstructed values of the 2000 ppm compartments are shown in Table 3. Because of the mis-positioning errors introduced, the standard deviation increased from 8.5% to 22% at an OCD of 0 mm. Other factors that affect the constructed results will be discussed in Sections 3.3 though 3.6. When the OCD increases from 0 to 9 mm, the deviation caused by mis-positioning increases from 22% to 28%. Therefore, the optimal off-center distance was chosen to be 0 mm for further investigation.

OCD (mm)	0	3	5	7	9
Deviation	22%	22%	23%	26%	28%

Table 3. Relative standard deviations caused by mis-positioning at different OCDs. For each of the OCDs from 0 to 9 mm, projection data for Distribution #1 in Table 1 were generated with mis- positioning distances (the distance between the center of the knee and the rotation axis of the system) of -2 mm, -1 mm, 0, 1 mm and 2 mm. The standard deviations of the reconstruction values of the 2000 ppm compartments are calculated.

3.3. The effect of variations in the outer dimensions of the knee

With other parameters fixed as described in Section 2.3, the outer dimensions of the knee were changed by 1 or 2 mm and projection data were generated assuming boron Distribution #1 in Table 1. Reconstructed values of boron concentration in each synovial compartment were then calculated using a

probability matrix, *A*, obtained using the original dimensions. The reconstruction results using the mismatching matrices are shown in Table 4. The relative standard deviation of the reconstructed values of the 2000 ppm compartments is 23%.

[B-10] (ppm)	100	2000	1000	2000	3000	2000	5000	2000
-2 mm	0	2574	1467	2820	4768	1672	7066	2447
-1 mm	0	2407	1090	2450	3750	1762	5310	2327
+0 mm	0	2114	915	2096	2994	1716	4116	2099
+1 mm	114	1732	834	1765	2413	1538	3406	1740
+2 mm	194	1411	823	1458	1960	1385	2827	1392

Table 4. The effect of reconstruction using a mis-matching probability matrix due to the variations in the outer dimensions of the knee. The outer dimension of the knee was increased or decreased by 1 or 2 mm to generate projection data of Distribution #1. The relative standard deviation of the reconstructed values of the 2000 ppm compartments is 23%.

3.4. The effect of variations in the depth of the synovium

With other parameters fixed as described in Section 2.3, the depth of the synovium was varied by 1 or 2 mm and projection data were generated assuming boron Distribution #1 in Table 1. Reconstructed values of boron concentration in each synovial compartment were then calculated using a probability matrix, *A*, obtained using the original synovium depth. The reconstruction results using the mismatching matrices are shown in Table 5. The relative standard deviation of the reconstructed values of the 2000 ppm compartments is 23%.

[B-10]	100	2000	1000	2000	3000	2000	5000	2000
-2 mm	0	2366	1809	2587	4983	1416	7999	2000
-1 mm	0	2297	1244	2383	3854	1614	5850	2099
+0 mm	0	2114	915	2096	2994	1716	4116	2099
+1 mm	270	1632	833	1769	2315	1515	3200	1704
+2 mm	396	1190	835	1405	1834	1276	2414	1341

Table 5. The effect of reconstruction using a mis-matching matrix due to the variations in the depth of the synovium. The depth of the synovium is varied by 1 or 2 mm to generate projection data of Distribution #1. The relative standard deviation of the reconstructed values of the 2000 ppm compartments is 23%.

3.5. The effect of off-center irradiations caused by positioning errors

With other parameters fixed as described in Section 2.3, the OCD was varied from -2 mm to 2 mm and projection data were generated assuming boron Distribution #1 in Table 1. Reconstructed values of boron concentration in each synovial compartment were then calculated using a probability matrix, *A*, obtained using an OCD of 0.0 mm, and shown in Table 6. The relative standard deviation of the

reconstructed values of the 2000 ppm compartments is 21%.

[B-10] (ppm)	100	2000	1000	2000	3000	2000	5000	2000
- 2 mm	172	2053	902	1364	3169	2313	3159	2729
-1 mm	92	2081	882	1695	3104	1954	3671	2384
+0	0	2114	915	2096	2994	1716	4116	2099
+ 1 mm	4.7	2076	960	2504	2734	1487	4586	1692
+ 2 mm	113	1898	1106	2851	2368	1480	4841	1270

Table 6. The effect of reconstruction using a mis-matching matrix due to off-center irradiation caused by positioning errors. The OCD was varied from -2 mm to 2 mm to generate projection data of Distribution #1. The relative standard deviation of the reconstructed values of the 2000 ppm compartments is 21%.

3.6. The effect of variations in the range of ^{10}B concentrations

With other parameters fixed as described in Section 2.3, projection data were generated for distributions that were proportional to the ^{10}B concentrations of Distribution #1, with a multiplying factor of 0.5, 1, 2 or 4. The total range of ^{10}B concentrations extend from 50 ppm to 10,000 ppm. The results are shown in Table 7, and reconstructed values vs. true ^{10}B concentrations are plotted in Figure 5.

[B-10](ppm)	100	2000	1000	2000	3000	2000	5000	2000
x 0.5	0	1232	482	1197	1795	1026	2661	1151
x 1	0	2114	915	2096	2994	1716	4116	2099
x 2	78	3415	1578	3316	4446	2769	5805	3375
x 4	318	4990	2453	4779	6015	3849	7281	4880

Table 7. The effect of variations in the range of ^{10}B concentrations. Projection data were generated for distributions that were proportional to the ^{10}B concentrations of Distribution #1, with a multiplying factor of 0.5, 1, 2 or 4. The total range of ^{10}B concentrations extends from 50 ppm to 10,000 ppm. Flux depression is observed at high ^{10}B concentrations.

3.7. The estimate of the reconstruction uncertainty

The uncertainty level of the IVPGNAA reconstruction is estimated by calculating the standard deviation of reconstructed values with combined offset parameters, which includes the

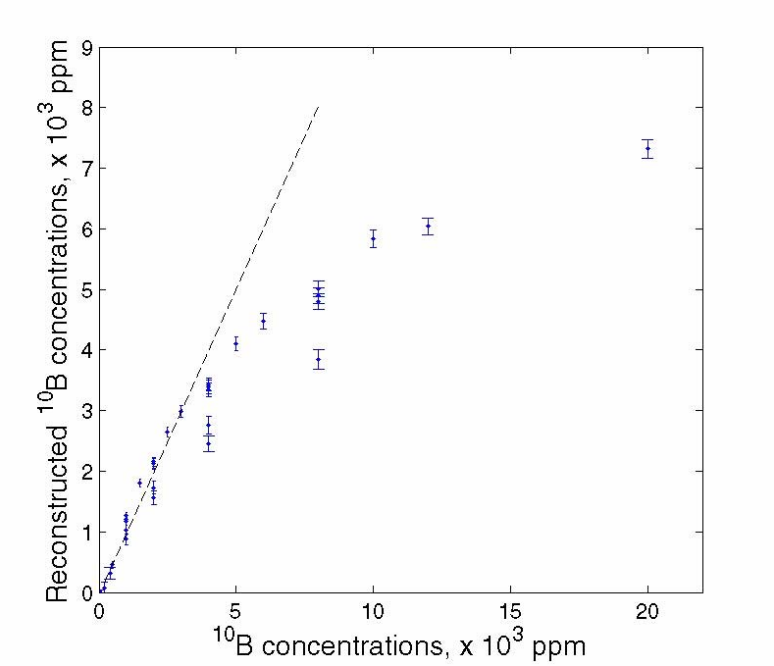

Figure 5. Plot of true versus reconstructed ^{10}B concentrations showing flux depression in IVPGNAA. At high ^{10}B concentrations, because of the strong absorption of neutrons by ^{10}B, the reconstructed results do not increase linearly with the ^{10}B concentrations. The dashed line shows the case without flux depression.

mis-positioning factors and variations in knee dimensions and the depth of the synovium. 13 sets of projection data were generated assuming Boron Distribution #1 in Table 1, with two or more parameters randomly selected to vary from those described in Section 2.3, with an offset of -2, -1, 1 or 2 mm. Reconstructed values of boron concentration in each compartment were then calculated using a probability matrix, A, obtained using the original parameters. The relative standard deviation of the reconstructed values of compartments with the same boron concentrations are used as an estimate of the reconstruction uncertainty. For a 2000 ppm concentration, the total number of compartments was 52, and the estimated uncertainty is 31%.

4. Summary of Preliminary Investigations of IVPGNAA

For IVPGNAA, a boronated compound will first be injected intra-articularly into an arthritic rabbit knee. The animal will then be secured on a rotatable stand with the knee positioned in a narrow neutron beam. A germanium detector will be used to collect the 478 keV prompt gamma photons from several angular positions. Projection data thus collected will then be reconstructed into a ^{10}B distribution map in the knee. This process will be repeated so that a time course of the compound migration pattern can be obtained. Only promising compounds showing long residence time and reasonably uniform distribution in the knee (synovium) during the screening procedure will be further investigated via dissection studies. The spatial resolution and quantification offered by IVPGNAA, although somewhat crude, represent valuable information useful in the determination of whether or not to continue evaluation of a given compound via more labor and cost intensive dissection studies.

Because information regarding the migration pattern of a compound from the synovial space to the synovium is highly desirable, a partition strategy which could distinguish ^{10}B in the synovium and synovial fluid is highly preferable. However, because the synovium is in immediate contact with the synovial fluid, the probability matrix of a distinguishing system tends to be singular. For example, a certain ^{10}B distribution pattern in the synovium compartments and a scaled version of this distribution in the synovial fluid compartments will yield similar projection data sets. Trial reconstructions using a distinguishing model confirmed that no consistent results can be obtained. Therefore, although highly preferable, the distinguishing model was rejected. As a consequence, information regarding the migration of a compound from the synovial fluid to the synovium is not available. However, other information, such as the residence time of the compound in the knee and the spatial distribution of the compound from the injection point to other regions of the knee, can still be obtained using the non-distinguishing model.

The MCNP simulation study presented here suggests that if the anatomical dimensions of the rabbit knee are available and there is no positioning error so that the probability matrix used in the reconstruction is a precise match to the experimental data acquisition, IVPGNAA coupled with NNWLS reconstruction can generate an accurate estimate of ^{10}B distribution in a rabbit knee with a 8.5% uncertainty. Additional errors up to 23% can be caused by mis-positioning or variations in anatomical dimensions among individual knees.

The reconstruction errors are estimated experimentally, by calculating the standard deviation of reconstruction values of the compartments with similar ^{10}B concentrations. In this simulation study, the estimated uncertainty for a 2000-ppm concentration is about 31%.

In actual animal experiments, the counting uncertainty of the projection data must also be considered. Therefore, the uncertainties of the reconstructed experimental results are expected to be higher. The magnitude of counting uncertainties will depend on some experimental conditions, such as the reactor power, the photon background level, and the efficiency of the detector to be used. From the relationship in Equation (3), it can be calculated that if the standard deviations of all the measurements are doubled, the error vector $\hat{x}_{WLS}$ is also doubled. In this simulation study, the uncertainty level of the projection data is approximately 5%. Therefore, if a counting uncertainty level of 10% or smaller is achievable in the animal experiments, the expected uncertainty of reconstructed values using a perfect-match matrix is estimated to be within 17%. When the effects of other factors are considered, including the mis-positioning errors and variations in knee anatomical dimensions, the estimated total uncertainty is within 40%.

From Figure 5 and Table 7, it can be seen that for high ^{10}B concentrations, the reconstructed values no longer increase linearly with ^{10}B concentration. This is due to neutron flux depression caused by the strong absorption of neutrons by ^{10}B, and can be corrected for by constructing a ^{10}B concentration calibration curve.

The difference in anatomical dimensions among individual knees may affect the result of

reconstruction. Table 4 shows that in trial reconstructions, a standard deviation of 23% for a 2000 ppm concentration can result from a variation of 1 to 2 mm in outer dimensions. Depending on the level of inflammation after the arthritis induction and the weight of the rabbits, the difference in the outer dimensions of AIA rabbit knees could be larger than 5 mm, which would cause reconstructed errors of larger than 23%. However, this effect can be eliminated by measuring the outer dimensions of each knee and pre-fabricating a probability matrix for each knee dimensions. In actual animal experiments, the outer dimensions of a knee can be obtained using vernier calipers.

Table 5 shows the effect of variations in the synovium depth on the reconstruction. In actual animals, the variation in the depth of the synovium is relatively small, usually within 2 mm. The depth of the synovium may be obtained via CT or MRI image, if available. Otherwise, the reconstruction will be performed using matrices obtained assuming varied synovial depths to give a range of possible distributions. The estimated variation caused by the difference in synovial depth is 23%.

In this simulation study, the boron containing region of the rabbit knee was partitioned into 8 compartments, and projection data were generated for 16 angular positions. With this configuration, when MITR is at full power (5 MW) and the initial injection contains 1.25 mg ^{10}B (0.25 ml of a 5000-ppm solution), the projection data for the reconstruction of one boron distribution map could be collected at the 4DH3 beam in 12 minutes with an expected uncertainty within 40% in reconstructed boron concentrations. In actual animal experiments, depending on the total boron concentrations injected and the migration pattern of a specific compound in the knee, different spatial/temporal resolutions might be desired, therefore the total compartment numbers and angular positions can be chosen accordingly.

The lower ^{10}B concentration limit of this approach will be determined by the counting uncertainty of the projection data, which will in turn be determined by the sensitivity of the IVPGNAA system, the photon background level, and the 478 keV photon acquisition time for each point. In actual animal experiments, this limit will also depend on how fast the compound to be screened will leave the knee. For a quickly dispersing compound, a higher temporal resolution is necessary, therefore a higher initial ^{10}B injection concentration is needed, otherwise the uncertainty level will be high. On the other hand, if a low uncertainty level is to be achieved without increasing the initial ^{10}B injection concentration, the temporal resolution must be compromised.

In summary, MCNP simulation studies demonstrated that IVPGNAA is feasible in providing crude information regarding the residence time of a ^{10}B labeled compound in a rabbit knee and its spatial distribution in different regions of the knee. When the irradiation conditions and the anatomical dimensions of the knee are precisely available, IVPGNAA is able to provide an estimate of ^{10}B concentrations in 8 regions of a rabbit knee within 10% uncertainty. This uncertainty reaches approximately 31% under realistic experimental conditions which would include mis-positioning errors and variations among individual knees. In actual animal experiments, additional errors are expected when counting uncertainties of raw projection data are taken into consideration. Although crude, information

provided by IVPGNAA is valuable in initial compound screening and for guidance of subsequent dissection studies.

5. Animal Experiments

The in vivo prompt gamma neutron activation analysis (IVPGNAA) was chosen for animal experiments. Three ^{10}B containing compounds were tested on AIA animal knees for their in vivo distribution behavior using the IVPGNAA approach. The results, when possible, are compared with previous dissection results.

5.1 Comparison of three approaches

Three approaches were proposed for the in vivo screening of ^{10}B in a rabbit knee: emission computed tomography (ECT), transmission computed tomography (TCT) and in vivo prompt gamma neutron activation analysis (IVPGNAA). The three approaches are compared for their spatial and temporal resolutions, and performance in ^{10}B quantification.

Theoretically, TCT has the potential of the best spatial resolution. Simulation results showed that when the pixel size of a reconstructed image is 1 mm, a spatial resolution of 2 mm can be obtained in regions with 2000 ppm ^{10}B. The temporal resolution of TCT will depend on the flux and energy distribution of the neutron source to be used. If a suitable source with sufficient intensity is available, the CCD camera exposure time can be as short as several seconds. In that case, it is possible to collect a complete set of projection data for one reconstruction in 10 minutes. It was shown that the neutron attenuation index map obtained with a TCT reconstruction can be directly related to a ^{10}B distribution in the knee. The quantification of both ECT and IVPGNAA is affected by two factors: the cross-talk between pixels (compartments) caused by neutron scattering, and the neutron flux suppression caused by the self-absorption of ^{10}B in the tissue. However, because TCT measures the transmitted neutron intensities directly, these two factors are less likely to affect TCT results. Therefore, TCT has the potential of the best performance for ^{10}B quantification.

The spatial resolution of ECT is expected to be inferior to TCT because the counting statistics with an emission tomography approach are usually worse than with a transmission tomography technique. In addition, more blurring can be caused by the high probability of neutron scattering in hydrogen – rich knee tissues. Simulation results showed that ^{10}B regions 5 mm in diameter can be successfully located under simulation conditions. The reconstructed 478 keV photon emission rate map is roughly proportional to local ^{10}B concentration. The most important drawback of ECT is that the data acquisition efficiency is significantly lower than that of TCT and IVPGNAA. Because the projection data have to be collected point by point in ECT, if projections from the same number of angular positions are collected, the acquisition time for ECT will be N times longer, where N is the number of data points in each projection. The system would also need to be automated, since the time for the manual operation of the stages is not negligible. If the 4DH1 beam port of MITR is used as the neutron source, the estimated time

for the collection of a complete projection data set for one reconstruction is one hour or longer.

IVPGNAA can be thought of as a simplified version of the ECT approach. Instead of collecting photons from several beam positions, IVPGNAA collects projections from only one point for each angular position. As a result, IVPGNAA has the crudest spatial resolution of all. However, simulation and phantom results showed that ^{10}B distributions in 8 regions can be reconstructed within reasonable data acquisition time, where the area of each region is approximately 40 mm^2. Similar to TCT, the temporal resolution of IVPGNAA mainly depends on the number of angular positions to be collected and the intensity of the neutron beam. If the MITR is at full power (leading a neutron flux level of 8.5×10^5 $cm^{-2}s^{-1}$ at the knee position), phantom experiments at the 4DH3 beam of MITR showed that a 12-minute data acquisition time is possible for a ^{10}B concentration range of several thousand ppm. Both ECT and IVPGNAA measure the secondary gamma emissions from ^{10}B capture reactions, therefore IVPGNAA is expected to have similar performance in ^{10}B quantification as ECT. Phantom experiments at the 4DH3 beam port of MITR showed that in IVPGNAA, regions with a ^{10}B concentration higher than 1000 ppm can be correctly located in the animal knee. The experimentally determined uncertainty level for the reconstructed results is 24.8% for a 2000 ppm concentration.

Comparing the three approaches, TCT has the best overall performance. However, the currently available neutron source (4DH3) does not have enough intensity for TCT, and the modification of other potential sources will involve considerable cost. Of the other two options, ECT has a better spatial resolution than IVPGNAA. But the temporal resolution of ECT is not acceptable due to its low data collection efficiency. Therefore IVPGNAA is chosen for the in vivo screening of ^{10}B in a rabbit knee.

5.2 Animal experiments at the 4DH3 beam port of MITR

Animal experiments were performed at the 4DH3 beam port of the MITR with three compounds: a boron particulate suspension in saline, a $K_2B_{12}H_{12}$ solution, and a $Na_2B_{10}H_{10}$ – liposome solution. When applicable, the IVPGNAA results were compared with previous dissection study results. Because of an emergency primary pump failure at the MITR, the experiments were carried out when the reactor was operating at half power (2.4 MW).

5.2.1 Uptake behaviors of compounds used in animal experiments

Three boronated compounds were chosen for the IVPGNAA animal experiments. Previous dissection studies showed that these three compounds have completely different uptake behavior in an AIA rabbit knee, therefore are good candidates to test the in vivo approach of ^{10}B analysis. The goal of the animal experiments is to test if IVPGNAA is able to detect the differences in uptake behavior among different compounds.

5.2.1.1 The $K_2B_{12}H_{12}$ solution

The $K_2B_{12}H_{12}$ solution is a typical fast-dispersing compound in the knee. When in solution, $K_2B_{12}H_{12}$ dissociates into 2 K^+ and one $B_{12}H_{12}^{2-}$ ions, which are quickly taken up by the synovium, followed by a fast depletion from the knee (Binello 1999).

In the dissection study of $K_2B_{12}H_{12}$, the initial injection was 0.25 ml of a solution with a boron concentration of 150,000 ppm, corresponding to an injection of 37.5 mg of boron in saline. Six rabbits were each sacrificed at 5, 15 and 30 minutes post injection, while three rabbits were sacrificed at 60 minutes. The knee joints were then carefully opened, and the synovial fluid, synovium and some other tissue samples such as the patella, tendon, ligament, menisci and bone chips were collected. The synovium samples were taken from four regions: the anterior, the posterior and two sides. The ^{10}B concentrations in those samples were later determined by PGNAA.

The dissection study showed that the synovium uptake quickly reached a very high level. The difference in uptake over the first 30 minutes was not statistically significant, and the time averaged uptake for the first 30 minutes was 19,000 ppm. The maximum standard deviation present at 5, 15 and 30 minutes was 50% of the mean. At 60 minutes, the average synovial concentration decreased significantly to about 37% of the concentration found between 5 and 30 minutes (Binello 1999).

Due to technical difficulties in the dissection studies, when the joint is opened, synovial fluid often spills out before it can be collected with a syringe. The amount of fluid recovered varied greatly among individual knees, so it is impossible to draw any conclusions about the total amount of boron in the fluid (Binello 1999). For this reason, the IVPGNAA results were compared with the average concentration of synovium uptakes in all three compounds for the comparison of uptake time courses. Because the residual boron in the fluid was not considered in the dissection study results, a certain extent of discrepancy between these two studies was expected.

5.2.1.2 The $Na_2B_{10}H_{10}$ – liposome solution

Liposomes are tiny fat-based spherical structures that can be produced from natural non-toxic phospholipids and cholesterol. These small artificial vesicles of spherical shape can be used as drug carriers and can be loaded with a great variety of molecules, such as small drug molecules, proteins, nucleotides and even plasmids. Liposomes have been used in the conventional treatment of RA for the delivery of steroid medications (McDougall 1980). The uptake behavior of the $Na_2B_{10}H_{10}$ salt is expected to be very similar to that of $K_2B_{12}H_{12}$; that is, it is a fast dispersing compound. However, when enclosed with a liposome vesicle, the dispersal rate can be greatly reduced, and the compound is expected to stay longer in the knee.

A $Na_2B_{10}H_{10}$ – liposome solution was prepared from $Na_2{}^{10}B_{10}H_{10}$ and Distearoylphosphocholine (DSPC) by Neutron Therapies, Inc. The solution contained 5810 ± 319 ppm of ^{10}B. The liposome size was 0.2μm (Wiersema 2002). In the dissection study, the initial injection was 0.25 ml of the solution, containing approximately 1.45 mg of ^{10}B. Two rabbits were each sacrificed at 1, 2 and 4 hours post

injection, and both knees of each rabbit (n = 4) were dissected.

As expected, the residence time of the liposome solution was significantly longer than that of $K_2B_{12}H_{12}$. The average synovium concentration at 1 hour post injection was 177 ppm, which decreased to 100 ppm after 2 hours, and 49 ppm after 4 hours. In each rabbit knee, four parts of the synovium were taken for ^{10}B determination: the anterior, the posterior, and two sides. The ^{10}B concentrations varied widely among different parts. While the average uptake concentration at one hour was 379 ppm for anterior synovium samples, the average posterior synovium uptake concentration was only 13.3 ppm, more than an order of magnitude lower than anterior samples. The uncertainty of ^{10}B determination ranged from 6.1% to 31%.

5.2.1.3 The boron particulate suspension

The boron particulate suspension contains 1 mg/ml of 99.9% boron metal in saline. The metal is 94% enriched in ^{10}B. The particles are spherical, with the diameter ranging from 5 to 40 μm. The average size is 15 μm (Johnson 1994). Therefore, the total ^{10}B concentration was 940 ppm.

In the dissection study, 0.25 ml of the suspension, containing 0.23 mg of ^{10}B, was injected into knees of three rabbits. Upon dissection, it was found that two of the rabbits were mis-injected, and a large coagulate of boron particulate was noticed in the muscle. In the one rabbit that was properly injected, the synovium uptake was very low, and a large coagulate was found in the synovial fluid. Because the boron particulate can easily coagulate in the synovial fluid, most of the compound stayed in the knee for a significantly longer time (longer than 24 hours) than the other two compounds. Only the boron particles that were separate from the coagulate were taken up by the synovium (Binello 1999). Therefore, the boron particulate suspension represents a type of compound that does not disperse in the knee.

5.2.2 Procedures for animal experiments

The IVPGNAA analyses of the three compounds described in Section 5.2.1 were conducted at the 4DH3 beam port of the MITR. To align the system, the back shielding wall and the sample holder of the PGNAA were temporarily removed. The laser pointer was slightly adjusted so that the laser beam pointed to the upper center of the 4DH3 beam opening. The collimator was placed at the back of the PGNAA shielding box. The collimator was positioned to line up the two slots with the laser beam. Next, the rotary table was adjusted so that the laser beam passed the center of the rotary table. The location of the rotary table was verified with a plummet, as shown in Figure 6(a). After the alignment, the 4DH3 neutron beam was opened, and the beam position was verified with a 4 mm × 4 mm (thickness × diameter) lithium iodine scintillation neutron detector.

Prior to the IVPGNAA analysis, both knees of three New Zealand white rabbits were made arthritic following the protocol of the AIA rabbit model. Before the IVPGNAA analysis, the animal was first anaesthetized with a mixture of 35 mg/kg (body weight) ketamine, 0.75 mg/kg acepromazine and 5

mg/ml xylazine. Each knee was then injected with 0.25 ml of the compound to be analyzed. The knee was subjected to several ranges of motions so that the compound distributed in the knee. The foot of the animal was fastened in a foot holder, as shown in Figure 6(b). The rabbit was then secured on the aluminum rabbit stand, as shown in Figure 6(c). The foot holder was inserted into the center of the rotary table, as shown in Figure 6(d), so that the knee was suspended in the neutron beam. The rotary table was turned to the orientation of the first angular position.

Prior to the data collection, the gamma acquisition time was preset. The acquisition time can be determined by the initial amount of ^{10}B injected and the reactor power at the time of experiments. The projection data collection was started immediately after the positioning of the animal. The neutron beam was opened, and a prompt gamma spectrum was collected for the first angular position. The area and uncertainty of the 478 keV peak were recorded, as well as the starting time of the acquisition. The rotary table was then turned 22.5º (m = 16) and a spectrum was collected for the second angular position. The process was repeated until most of the compound left the knee, or the total acquisition time exceeded 3 hours. Additional anesthesias in half doses were given when the animal showed signs of gaining consciousness.

After the data collection, the neutron beam was turned off and the animal was removed from the stand. The outer dimensions of the knee were measured with vernier calipers. The collimator was removed, and the back shielding wall and the sample holder of the PGNAA facility were restored.

To reconstruct the in vivo ^{10}B distribution, first a probability matrix for each knee was generated with MCNP simulations using the model shown in Figure 3. The measured outer dimensions and a synovium depth of 3 mm along the short axis were used in generating the matrix. The boron-containing portion of each knee was divided into 8 sections (n = 8), as shown in Figure 4. The ^{10}B distributions were then reconstructed using the NNWLS algorithm.

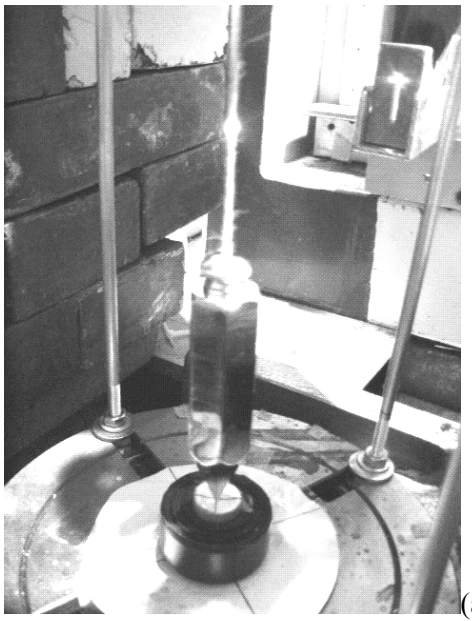

(a)

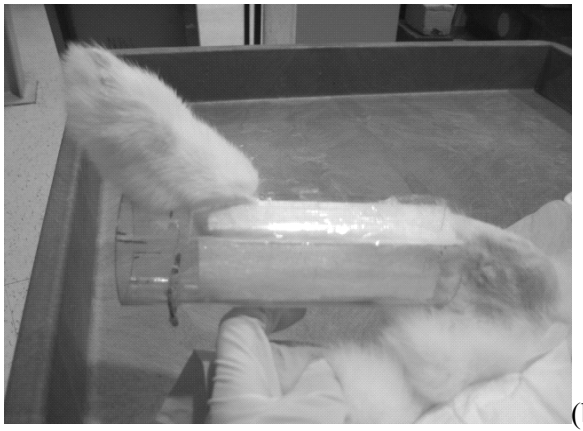

(b)


(c)


(d)

Figure 6 Positioning of the rabbit knee for IVPGNAA analysis. (a) The position of the rotary table was verified with a plummet. (b) The foot of the animal was fastened into the foot holder after the initial injection of the compound. (c) The animal was placed on the aluminum stand. The body can be fastened with tapes if necessary. (d) The foot holder was inserted into the center of the rotary table so that the animal knee was suspended in the beam.

5.2.3 The IVPGNAA reconstruction results of three compounds

Raw projection data were collected for varied lengths of time for the three compounds described in Section 5.2.1. Because of the variations in the volumes of the synovial tissue and fluid between different animals, it is difficult to obtain the absolute ^{10}B concentrations. Therefore, all reconstruction results for each knee were normalized in such a manner that the total amount of ^{10}B in all the compartments was assumed to be 8 units for the first round of data collection. The total volume of the synovium and synovial fluid of the knee model shown in Figure 3 was 1.69 ml. Therefore, a crude estimate of the concentration can be made by assuming the volume of each compartment is 0.21 ml. The total reconstructed values in all the compartments were summed up for each round of reconstruction. The sums were then plotted versus the time points of data collection, as an indication of the residence time course of the compound in the knee.

5.2.3.1 The $K_2B_{12}H_{12}$ solution

The $K_2B_{12}H_{12}$ solution used was freshly made with 124,000 ppm natural boron in saline. The ^{10}B concentration was then 23,350 ppm. One knee was used in the analysis of $K_2B_{12}H_{12}$. The acquisition time for each data point was 40 seconds. The data collection lasted for approximately 1.5 hours. A total of 5 projection data sets were collected. The reconstructed results are shown in Table 8 and Figure 7. It can be seen that the compound leaves the knee rapidly. About half of the compound left the knee by approximately one hour after the injection. A small extent of compound migration can be observed.

The total reconstruction value versus data collection time curve is plotted in Figure 8(a). The results of ^{10}B uptake concentrations in the synovium via previous dissection study (Binello, 1999) are

shown in Figure 8(b) for comparison. The dissection studies showed that there was no statistically significant difference in uptake over the first 30 minutes: the time averaged uptake was 19,000 ppm. By 60 minutes, the average synovial concentration decreased significantly to about 37% of the concentration found between 5 and 30 minutes.

Post-injection time (mid-point) , min	Compartment #								
	1	2	3	4	5	6	7	8	Total
4 – 18 (11)	1.4	0.16	5.1	0	0	0	0	1.3	8.0
18 – 34 (26)	0.40	0	4.7	0.0	0	0	0	2.0	7.1
34 – 47 (40.5)	0.66	0	3.9	0.12	0	0	0.72	1.3	6.7
47 – 70 (58.5)	0.59	0	2.9	0.20	0	0	0	0.71	4.4
70 – 84 (77)	0	0.93	1.3	0	0	0	0	0.04	2.3

Table 8 The IVPGNAA results following injection of 0.25 ml $K_2B_{12}H_{12}$ solution containing 124,000 ppm of boron. The reconstruction results are also shown as images in Figure 7. The reconstructed values were normalized by assuming an initial injection amount of 8 units. About half of the compound left the knee at around one hour after the injection. A small extent of compound migration is observed.

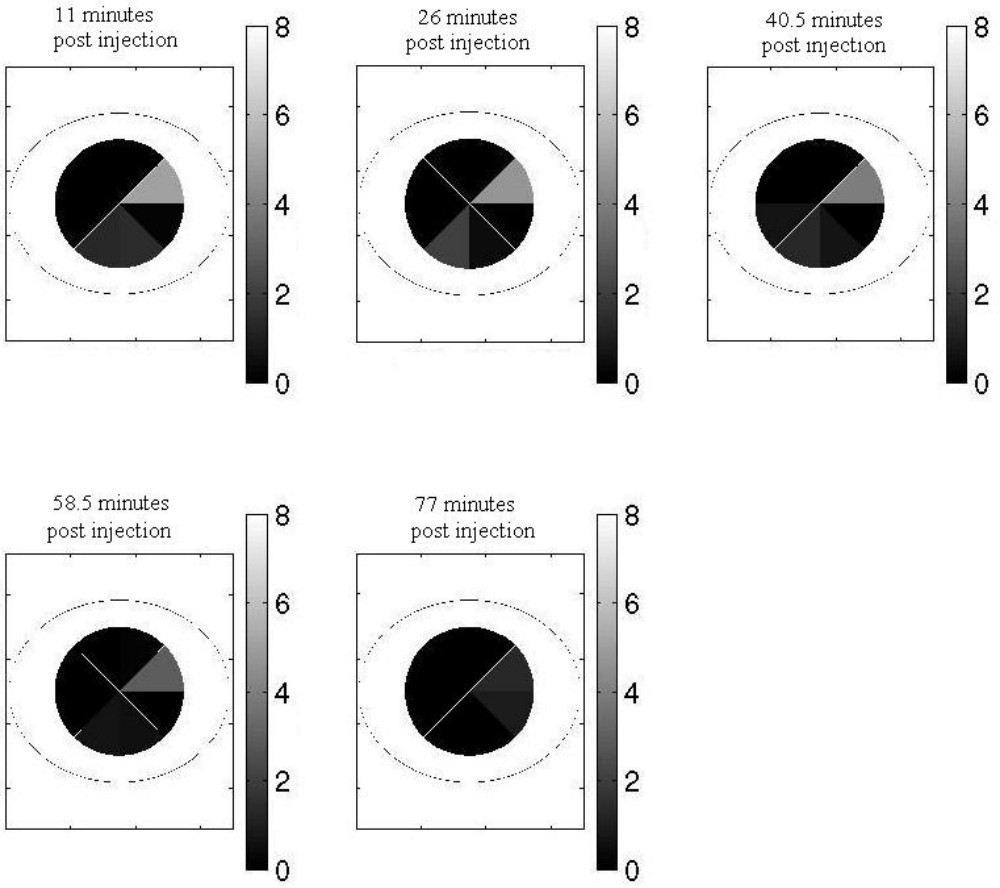

Figure 7 The images of the reconstructed results shown in Table 8. Relative units.

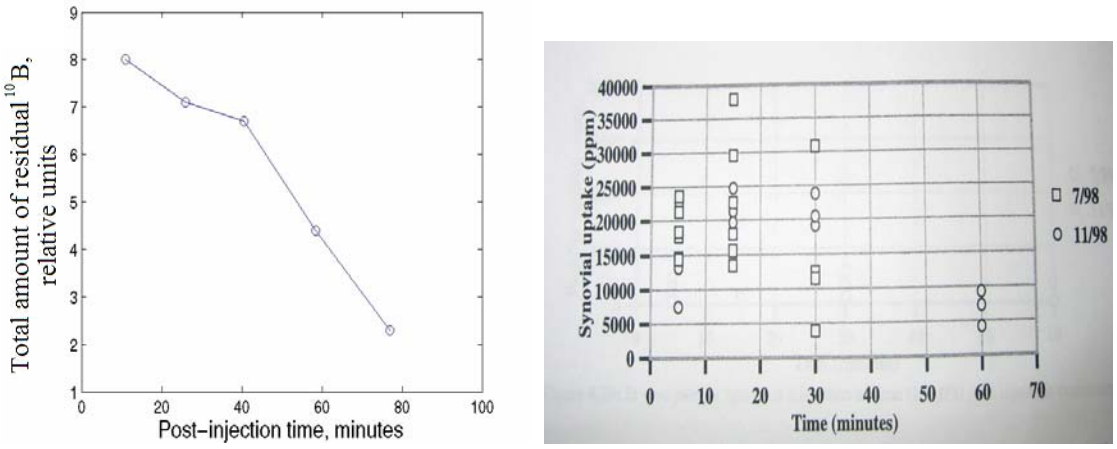

(a) (b)

Figure 8 Comparison of the IVPGNAA and dissection results of the $K_2B_{12}H_{12}$ uptake behavior. (a) The IVPGNAA result that shows the relative decrease of the total amount of ^{10}B in the knee as a function of the post injection time. (b) The dissection study result that shows the synovial uptake concentrations as a function of time, as measured by PGNAA (Binello 1999).

Compared with the dissection result, the residence time of $K_2B_{12}H_{12}$ obtained using the in vivo approach was slightly longer. The total amount of residual boron at 60 minutes was approximately 64% of the average amount found during the first 40 minutes. Because the synovial fluid can not be completely recovered in the dissection studies, a certain extent of discrepancy is expected when the results are compared with the IVPGNAA results. Another possible reason is that in the dissection study, an animal was sacrificed at the specified time point, and the knee was dissected afterwards. However, approximately 10 minutes are needed for the dissection of each knee. After sacrifice of the animal, the voluntary phagocytic process and the circulation were stopped, but diffusion can still happen during the time interval between the sacrifice of the animal and the dissection. Taking this factor into consideration, the IVPGNAA result was a reasonable indication of the residence time of this compound in the knee.

5.2.3.2 The $Na_2B_{10}H_{10}$ – liposome solution

The $Na_2B_{10}H_{10}$ – liposome solution used was the same as the one used in the dissection study. The solution contained 5810 ± 319 ppm of ^{10}B, and the liposome size was 0.2 □m. The liposome sample was tested on two knees. The acquisition time for each data point was 90 seconds. The data collection lasted for approximately 3 hours. A total of 7 projection data sets were collected for the first knee, and 8 projection data sets were collected for the second knee. The reconstructed results are shown in Tables 9 and 10, and as images in Figures 9 and 10. It can be seen that the compound stayed in the knee longer than $K_2B_{12}H_{12}$. In both knees, less than 50% of the compound had left by 2 hours after the injection. The total reconstruction values versus data collection time are plotted in Figure 11. Also shown in Figure 11 is

the synovium uptake time curve of the liposome sample obtained by dissection study.

The dissection study showed that the average synovium concentration at 1 hour post injection was 177 ppm, which decreased to 100 ppm after 2 hours, and 49 ppm after 4 hours. In each rabbit knee, four parts of the synovium were taken for ^{10}B determination: the anterior, the posterior, and two sides. The ^{10}B concentrations varied widely among different regions of the synovium. The average anterior synovium uptake concentration was more than an order of magnitude higher than the average posterior uptake concentration, which suggests that the compound did not migrate very much from the injection point.

Post-injection time (mid-point) , min	Compartment #								
	1	2	3	4	5	6	7	8	Total
7 – 37 (22)	0	6.0	2.0	0	0	0	0	0	8.0
37 – 57 (47)	0	5.9	1.9	0	0	0	0	0	7.8
57 – 78 (67.5)	0	4.0	1.6	0	0	0	0	0	5.6
78 – 97 (87.5)	0	5.9	0	0	0	0	0	0	5.9
97 – 118 (107.5)	0	3.7	1.3	0	0	0	0.19	0	5.2
118 – 152 (135)	0	5.2	0	0	0	0	0	0	5.2
152 – 184 (168)	0	3.8	1.0	0	0	0	0	0	4.8

Table 9 The IVPGNAA results following injection of 0.25 ml $Na_2B_{12}H_{12}$ – liposome solution containing 5810 ppm ^{10}B: the first knee. The reaults are also shown as images in Figure 9. The reconstructed values were normalized by assuming an initial injection amount of 8 units. Less than 50% of the compound left the knee by two hours after the injection.

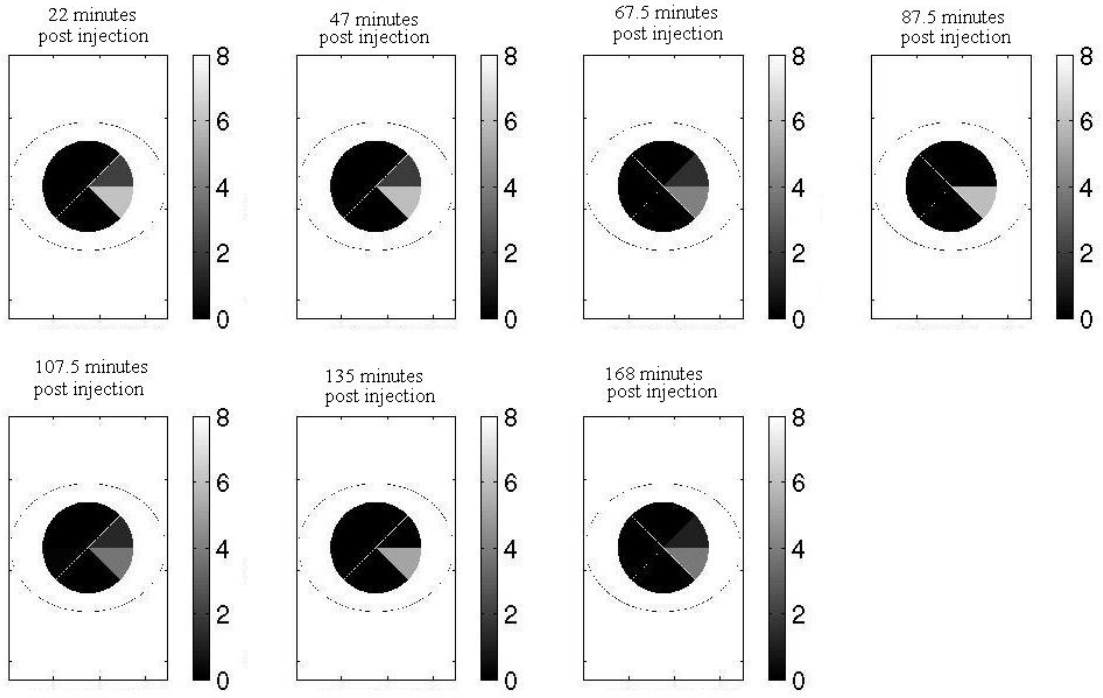

Figure 9 The images of reconstructed results shown in Table 9. Relative units.

Post-injection time (mid-point) , min	Compartment #								
	1	2	3	4	5	6	7	8	Total
5 – 25 (15)	0	8	0	0	0	0	0	0	8
25 – 45 (35)	0	6.1	0	0	0	0	0	0	6.1
45 – 65 (55)	0	4.3	0	0	1.0	0.5	0	0	5.8
65 – 86 (75.5)	0	4.1	0	0	0	0.2	0	0	4.3
86 – 109 (97.5)	0	1.8	3.1	0	0	0	0	0	4.9
109 – 135 (122)	0	2.3	2.0	0	0	0	0	0	4.3
135 – 150 (142.5)	0	2.4	1.6	0	0	0.9	0	0	4.5
150 – 171 (160.5)	0	2.5	0.6	0	0	0	0	0	3.1

Table 10 The IVPGNAA results following injection of 0.25 ml $Na_2B_{12}H_{12}$ – liposome solution containing 5810 ppm ^{10}B: the second knee. The reconstructed results are also shown as images in Figure 10. The reconstructed values were normalized by assuming an initial injection amount of 8 units. Less than 50% of the compound left the knee by two hours after the injection.

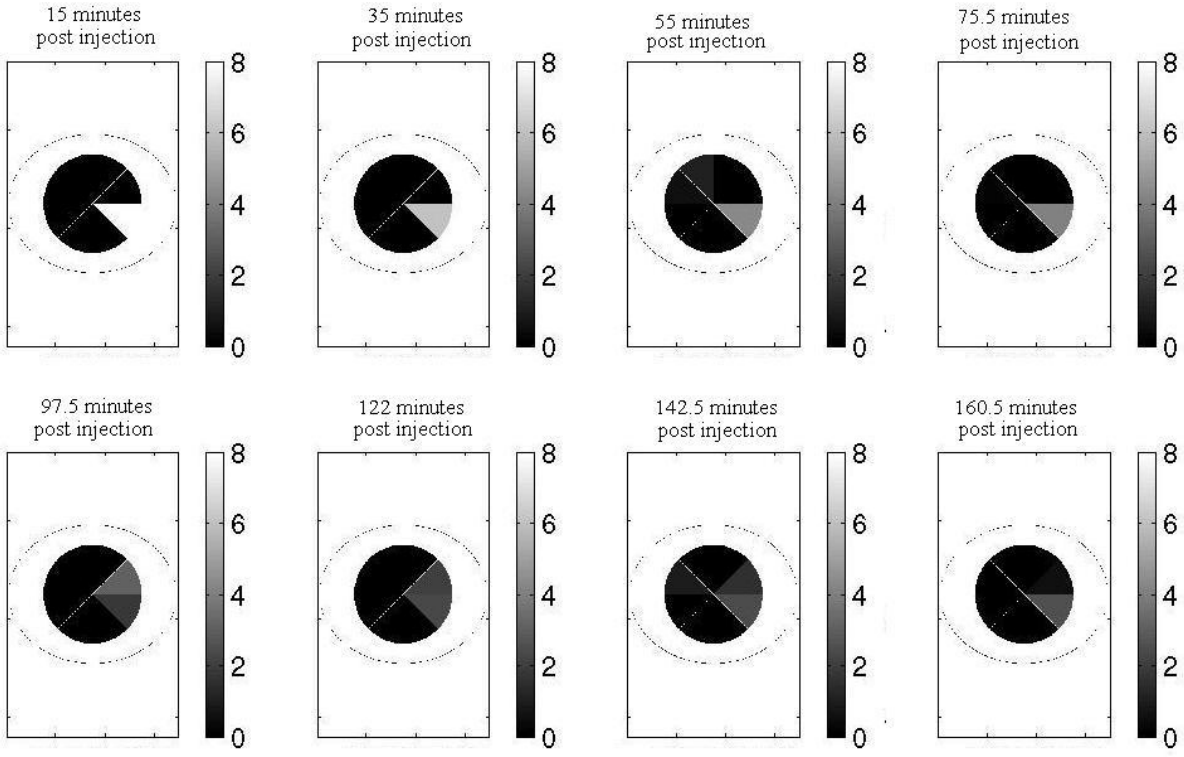

Figure 10 The images of reconstruction results shown in Table 10. Relative units.

Compared with the dissection results, the rate that the liposome sample leaves the knee obtained via IVPGNAA is also lower than that of the dissection study, but the difference is somewhat smaller

compared with the $K_2B_{12}H_{12}$ compound. Therefore, it is possible that less of the liposome sample leaves the knee by diffusion, and more by a voluntary phagocytic process. This is a reasonable guess, because the size of a liposome vesicle (0.2 μm) is significantly larger than the size of an ion (~10^{-9} to 10^{-10} cm). From Tables 9 and 10, very little migration of the compound was observed. This is consistent with the results of the dissection studies.

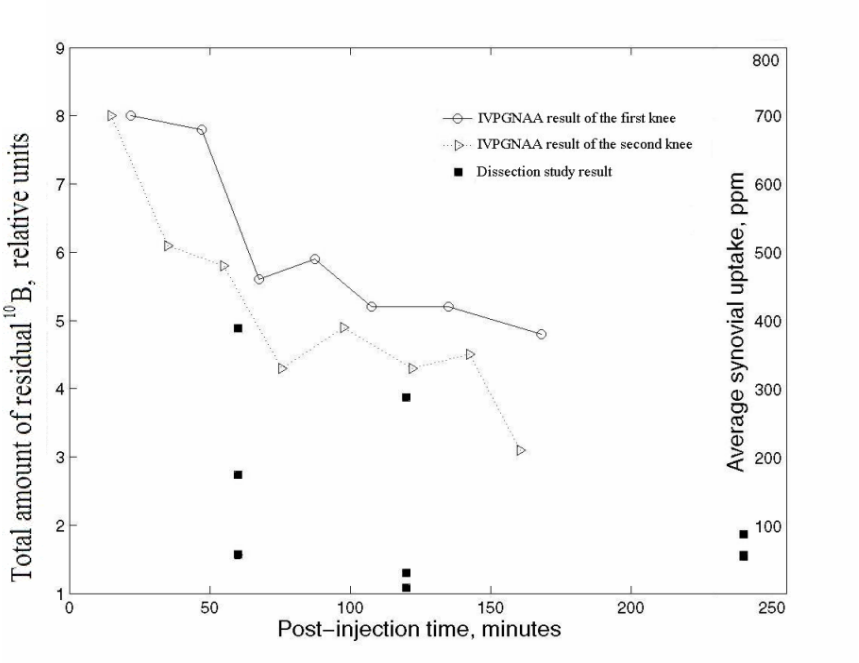

Figure 11 Comparison of the IVPGNAA and dissection results of the $Na_2B_{12}H_{12}$ – liposome uptake behavior. The IVPGNAA results are shown as the relative decrease in the total amount of ^{10}B in the two knees as a function of the post injection time. The dissection study results are shown as the synovial uptake concentrations as a function of post-injection time, as measured by PGNAA.

5.2.3.3 The boron particulate suspension

The boron particulate suspension used in the IVPGNAA analysis was the same as the one used in the dissection study. The total ^{10}B concentration was 940 ppm. Because the reactor was operating at half power and the ^{10}B concentration of the suspension was low, the acquisition time was preset to 5 minutes for each data point. However, even so the statistical uncertainty of gamma acquisition was higher than 30% at all data points. Therefore, no meaningful reconstructions were obtained.

One possible reason was the low neutron intensity caused by the half power operation of MITR. Procedures described in Section 5.4.4 were performed at half power to determine the detection limit. The sensitivity of the system was measured to be 16.1 ± 0.8 cps/mg ^{10}B. The background count rate under the ^{10}B peak was 23.0 ± 0.1 cps. With a 5-minute gamma acquisition time, the ^{10}B concentration of the initial injection should be no lower than 912 ppm, which was close to the boron concentration of the available suspension, 940 ppm.

However, previous dissection study results revealed that boron particulate coagulates in the synovial fluid and does not enter the synovium. As demonstrated above, ^{10}B in the synovial fluid can only provide approximately half the useful gamma signals provided by ^{10}B in the synovium. In fact, an estimated initial injection concentration of 1986 ppm was necessary for compounds staying in the fluid space. Therefore, the inability to detect the compound via IVPGNAA suggested the possibility that the compound stayed in the synovial fluid and did not migrate into the synovium. This is consistent with the results of the dissection studies.

5.2.3.4 Estimation of the uncertainty level of the animal experiment

As stated in Section 3.6, the sources of errors in IVPGNAA include: statistical uncertainties associated with the 478 keV gamma counting, reconstruction errors, mis-positioning errors, and discrepancies in the parameters (the outer knee dimensions and the depth of the synovium) assumed for the generation of the probability matrix. The uncertainty associated with reconstruction results comes from the combination of these effects.

In the phantom experiments, the uncertainty of a 2000 ppm ^{10}B concentration in a 40 mm^2 region was experimentally estimated to be 24.8%. The gamma counting uncertainty of most data points was in the range of 5% to 15% in the phantom experiments except for points with extremely low ^{10}B concentrations (less than 1000 ppm) . In the animal experiments, the gamma counting uncertainty increased to 8% to 30% for $K_2B_{12}H_{12}$, and from 10% to 40% for the liposome solution. In addition, the mismatch of the synovial depth in the generation of the probability matrix was inapplicable in the phantom experiments, but presented in the animal experiments, since the actual synovial depth in a rabbit knee can not be readily measured.

The component of uncertainty caused by gamma counting statistics and the reconstruction process can be estimated using the property of the error vector of the reconstruction algorithm. It can be calculated that if the standard deviations of all the measurements are doubled, the error vector $\hat{x}_{WLS}$ is also doubled. In the simulation study, when the gamma counting uncertainty was approximately 5%, the uncertainty level of a 2000 ppm concentration in a 40 mm^2 region was estimated to be 8.2%. Therefore, that component of uncertainty caused by counting statistics and reconstruction errors was estimated to be 13.1% for $K_2B_{12}H_{12}$, and 16.4% for the liposome solution. The total uncertainty level was estimated to increase to 26.8% and 28.6% for $K_2B_{12}H_{12}$ and the liposome solution, respectively. In the simulation study, it was shown that the variation in the synovium depth within ± 2 mm can cause the uncertainty of reconstruction to increase from 8.2% to 25%. This factor will cause the uncertainty level to increase to 35.7% and 37.2% for $K_2B_{12}H_{12}$ and the liposome solution, respectively.

5.3 Summary of the animal experiments

IVPGNAA was tested on live AIA rabbit knees with three boronated compounds with vastly

different uptake behavior: a $K_2B_{12}H_{12}$ solution, a 0.2 μm $Na_2B_{10}H_{10}$-liposome solution and a boron particulate suspension. Because of an emergency primary pump failure, MITR was operating at half power when the animal experiments were conducted.

For each compound, several projection data sets were collected over a time course of 1.5 to 3 hours after the knee injection. The ^{10}B distributions were reconstructed and the compound egress time courses were compared with the dissection study results. For the $K_2B_{12}H_{12}$ and the liposome solutions, the compound residence times obtained via IVPGNAA were slightly longer than the results of dissection studies. Because it is difficult to recover all the synovium fluid in the dissection studies, a discrepancy between the dissection study results and the IVPGNAA results was expected. This discrepancy can be further explained by the time delay between the sacrifice and dissection of the animal in the dissection studies. For the boron particulate suspension, the ^{10}B concentration of the available compound was close to and slightly higher than the detection limit, but the statistic uncertainties of the gamma counting were still too high to provide meaningful results. This suggested that the compound stayed in the synovial fluid space, therefore could not contribute as much gamma signals as it would if the compound dispersed into the synovium. This agreed with the results of the dissection study.

5.4 A protocol of IVPGNAA for the in vivo screening of ^{10}B in a rabbit knee

This section summarizes the procedures for the IVPGNAA screening of ^{10}B in an AIA rabbit knee as developed in this work.

1. The preparation of the animal. Induce AIA arthritis in the knees of the New England White rabbit. Before the arthritis induction, intramuscularly inject the animal with a mixture of 35 mg/kg (body weight) ketamine, 0.75 mg/kg acepromazine and 5 mg/ml xylazine for anesthesia. After the knee induction, a subcutaneous injection of 0.02 to 0.05 mg/kg (body weight) buprenorphine should be given to the animal every 12 hours until the signs of pain and distress disappear.
2. Alignment of the system. Remove the back shielding wall and the sample holder of the PGNAA facility. Slightly adjust the laser pointer so that the laser beam points to the upper center of the 4DH3 beam opening. Place the collimator at the back of the PGNAA shielding box. Adjust the collimator to align the two slots with the laser beam. Adjust the rotary table so that the laser beam passes the center of the rotary table. Verify the location of the rotary table with a plummet, as shown in Figure 6(a). Open the neutron beam and verify the beam position with a lithium iodine scintillation neutron detector. Calibrate the high purity germanium gamma spectrum system and preset the gamma ray acquisition time.
3. Positioning of the animal. Anaesthetize the animal using the same mixture described in Step 1. Inject 0.25 ml of the compound to be screened intra-articularly into one knee. Subject the knee to several ranges of motions so that the compound distributes in the knee. Fasten the foot of the animal in the

foot holder, as shown in Figure 6(b). Secure the animal on the aluminum rabbit stand, as shown in Figure 6(c). Insert the foot holder into the center of the rotary table, as shown in Figure 6(d), so that the knee is suspended in the neutron beam. Turn the rotary table to the orientation of the first angular position.

4. Projection data collection. Open the neutron beam. Collect the gamma spectrum for the first angular position. Record the area and uncertainty of the 478 keV peak, and the starting time of the acquisition. Turn the rotary table 22.5º (m = 16) and repeat the process for the second angular position. Repeat the process until most of the compound leaves the knee, or the total acquisition time exceeds 3 hours. Additional anesthesia in half dose should be given when the animal shows signs of gaining consciousness.
5. Restoration of the PGNAA facility. After data collection, turn the neutron beam off and remove the animal from the stand. Measure the outer dimensions of the knee with vernier calipers. Remove the collimator and restore the back shielding wall and the sample holder of the PGNAA facility.
6. Reconstruction. Generate a probability matrix for each knee with MCNP simulations using the model shown in Figure 3. Use the measured outer dimensions and a synovium depth of 3 mm along the short axis. Reconstruct ^{10}B distributions using the NNWLS algorithm. Normalize the reconstructed results assuming the total amount of ^{10}B in the first round is 8 units. Evaluate the spatial dispersion of the compound by observing the change in relative boron amounts in the compartments. Plot the total reconstructed value of each round versus the midpoint of the time of acquisition as a time course of the compound dispersion.

5.5 Project Conclusion

The results of the phantom and animal experiments showed that IVPGNAA is a feasible approach for the in vivo screening of ^{10}B in a rabbit knee. ^{10}B distributions in 8 regions of the knee can be estimated via the reconstruction process. Regions of high ^{10}B concentrations can be correctly located in the knee. Raw projection data for each reconstruction can be collected within 12 minutes when the MITR is operated at full power, provided the ^{10}B concentration of the initial injection is higher than 4180 ppm. The compound residence time course obtained by IVPGNAA is a correct reflection of the compound egression process. It can be concluded, therefore, that IVPGNAA can be used as a useful tool for the guidance of dissection studies in the evaluation of potential compounds for BNCS.

6 References

Binello E 1999 Efficacy of Boron Neutron Capture Synovectomy in an Animal Model *PhD Thesis* Department of Nuclear Engineering, Massachusetts Institute of Technology, USA

Briesmeister JF 1997 MCNP - A general Monte Carlo N-Particle Transport code, Version 4B. *Los Alamos National Laboratory Report, LA - 12625 - M* (Los Alamos)

Harris E D, Jr. 2001 Treatment of rheumatoid arthritis *Kelley's Textbook of Rheumatology, 6th Ed.* ed Ruddy S, Harris E D, Jr. and Sledge C B (Philadelphia, Pennsylvania: W. B. Saunder) pp 1001-22

ICRU1989 Tissue Substitutes in Radiation Dosimetry and Measurement *International Commission on Radiation Units and Measurements Report 44* (Bethesda, Maryland: ICRU)

Lanza R C, Shi S and Mcfarland E W 1996 A cooled CCD based neutron imaging system for low fluence neutron sources *IEEE trans. Nucl. Sci.* **43** 1347-51

Lawson C L and Hanson R J 1974 Solving Least Squares Problems (Englewood Cliffs, New Jersey: Prentice-Hall)

Newman A P 1994 Synovectomy *Arthritis Surgery* ed Sledge C B, Ruddy S, Harris E D, Jr. and Kelley W N (Philadelphia, Pennsylvania: W. B. Saunder)

Newton T, Riley K J and Harling O K 2002 Development and implementation of procedures used in clinical trials of BNCT at the MIT Nuclear Reactor 1*0th International Congress on Neutron Capture Therapy (Essen, Germany, 8-13 September 2002)* pp 203-6

Riley K J and Harling O K 1998 An improved prompt gamma neutron activation analysis facility using a focused diffracted neutron beam *Nucl. Instr. and Meth. in Phys. Res. B* **143** 414-21

Shortkroff S, Binello E, Zhu X, Gierga D, Thornhill T S, Shefer R and Yanch J C 2003 Dose response to boron neutron capture synovectomy of the AIA rabbit stifle joint *Accepted by Nuclear Medicine and Biology*

Shortkroff S, Jones A G and Sledge C B 1993 Radiation synovectomy *Advances in Metals in Medicine Vol. 1* (Greenwich, Connecticut: JAI Press Incorporated)

Strang G 1986 Introduction to Applied Mathematics (Wellesley, Massachusetts: Wellesley-Cambridge Press)

Yanch J C, Shortkroff S, Shefer R E, Johnson S, Binello E, Gierga D, Jones A G, Young G, Vivieros C, Davison A and Sledge CB 1999 Boron neutron capture synovectomy: Treatment of rheumatoid arthritis based on the $^{10}B(n,\square)^{7}Li$ nuclear reaction *Med. Phys.* **26** 364-75

Zhu X, Yanch J C and Shortkroff S 2002 In vivo screening of ^{10}B compounds of potential use in Boron Neutron Capture Synovectomy 1*0th International Congress on Neutron Capture Therapy (Essen, Germany, 8-13 September 2002)* pp 891-5